Clinical Oral Implants Research

WILEY

CLINICAL ORAL IMPLANTS RESEARCH

ORIGINAL ARTICLE OPEN ACCESS

In Vitro Assessment of a Novel Piranha-Passivated Dental Implant Surface Against Oral Biofilm Formation

Paula Nuevo[1] | Leire Virto[1,2] | Honorato Ribeiro-Vidal[3,4] | Javier Gil[5] | Mariano Sanz[1]

[1]ETEP (Etiology and Therapy of Periodontal and Peri-Implant Diseases) Research Group, Faculty of Dentistry, Complutense University, Madrid, Spain | [2]Department of Anatomy and Embriology, Faculty of Optics and Optometry, Complutense University, Madrid, Spain | [3]Specialization in Periodontology and Implants, Faculty of Dental Medicine, University of Porto, Porto, Portugal | [4]LAQV/REQUIMTE, University of Porto, Porto, Portugal | [5]Bioinspired Oral Biomaterials and Interfaces, Department of Ciencia e Ingeniería de Materiales, Escola d'Enginyeria Barcelona Est, Technical University of Catalonia, Barcelona, Spain

Correspondence: Leire Virto (lvirto@ucm.es)

Received: 7 March 2025 | **Revised:** 3 July 2025 | **Accepted:** 13 August 2025

Funding: This research was supported by Cátedra Extraordinaria Klockner de investigación básica y aplicada en implantes dentales.

Keywords: dental meshes | multispecies biofilm | passivation | peri-implantitis | piranha | titanium

ABSTRACT

Background and Objectives: Peri-implantitis, a significant complication resulting from bacterial colonization on dental implants, presents a challenge in oral healthcare. Developing surfaces that inhibit bacterial adhesion while promoting tissue integration is crucial for improving implant outcomes. This study aims to evaluate bacterial colonization on a novel passivated surface for dental implants using an in vitro multispecies biofilm model.

Materials and Methods: Three types of titanium implants (standard, citric acid-passivated, and piranha-passivated) were characterized by analyzing roughness, contact angle values, and surface energy after the passivation treatments. The capacity for biofilm formation on these implants was evaluated using quantitative polymerase chain reaction (qPCR), scanning electron microscopy (SEM), and confocal laser scanning microscopy (CLSM). Bacterial colonization and viability were assessed at 6, 12, and 24 h. In addition, the protein adsorption capacity of these surfaces was determined.

Results: Treatments increased hydrophilicity and polar surface energy, with no change in roughness. Although no statistically significant differences were found, a slightly lower concentration of primary and intermediate colonizers was observed on piranha-treated surfaces compared to citric acid implants, particularly during the 24-h incubation period. CLSM analyses revealed a higher percentage of dead bacteria on piranha-passivated implants over time. Piranha passivation also resulted in the lowest fibrinogen adsorption.

Conclusion: These findings suggest that piranha passivation may be a promising treatment for dental implant surfaces, potentially reducing the risk of peri-implantitis. However, the inherent limitations of the in vitro approach necessitate further clinical trials to validate the efficacy of this surface modification in real-world clinical settings.

1 | Introduction

Dental implants are considered a reliable solution for addressing edentulism, offering patients enhanced functionality, aesthetics, and overall quality of life (Chatzopoulos and Wolff 2024). Despite their high success rates, peri-implant diseases remain the most common complication (Rokaya et al. 2020), with approximately 29.48% (implant-based) and 46.83% (subject-based) of dental implants experiencing peri-implant mucositis (Lee et al. 2017), while about 11.5% (implant-based) and 20%

(subject-based) develop peri-implantitis (Diaz et al. 2022). These complications not only threaten the success of implants but also impose significant health and economic burdens on patients and healthcare systems (Fragkioudakis et al. 2021). The formation and maturation of biofilms on dental implant surfaces have been associated with the onset and progression of these diseases (Belibasakis et al. 2015; Busscher et al. 2010; Lang and Berglundh 2011; Lee and Wang 2010). In fact, their treatment depends on biofilm removal through the decontamination of the implant surface, using either nonsurgical or surgical methods (Rokaya et al. 2020).

Since bacterial adhesion occurs immediately after implant placement, innovative surface technologies involving texturing, hydrophilization, and chemical functionalization are being developed not only to enhance protein adsorption, cell adhesion, and proliferation (Kunrath et al. 2024), thereby promoting better bone–implant contact and accelerating the osseointegration process, but also to provide antibacterial properties that inhibit biofilm formation (Esteves et al. 2022).

One approach involves applying coatings with antimicrobial properties to the surface of implants, including antibiotics and antimicrobial peptides; however, safety concerns and their long-term effectiveness present challenges. Another strategy has been to modify surface topography to minimize bacterial adhesion, as bacteria can sense and respond to chemical and mechanical signals from implant surfaces (Zhai et al. 2023). One such method, passivation, entails an oxidation reaction that enhances the implant surface topography by forming a highly hydrophilic protective layer with a negative charge, which promotes osteoblast differentiation, proliferation, and the production of extracellular matrix components (Cruz et al. 2020). A novel passivation technique (Piranha) employs a solution mixture of sulfuric acid and hydrogen peroxide to create surfaces with distinct nanotexture and chemical properties; however, its impact on microbial colonization remains understudied (Cruz et al. 2022). Therefore, this in vitro investigation seeks to evaluate the effect of this novel surface on biofilm formation using a multispecies dynamic subgingival biofilm model.

2 | Material and Methods

Considering the in vitro nature of the investigations, which did not involve human or animal subjects or material, no ethical review was required.

2.1 | Material Specimens

The dental implants are made of commercially pure grade 3 titanium manufactured by Klockner Medical Group (Escaldes Engordany, Andorra). They are bone-level implants of 4 mm in diameter and 10 mm in length, with a moderately rough surface. Three different surface topographies were used.

- Standard implants as the negative control.
- Passivated with 25% v/v citric acid for 120 s as the positive control (Vilarrasa et al. 2023, 2025).
- Test implants utilizing the new passivation method (Piranha) (Klockner. Spain, based on immersion in sulfuric acid and hydrogen peroxide for 2 h).

The surfaces obtained through scanning electron microscopy can be seen in Figure 1. The three surfaces were characterized for their roughness values using confocal microscopy, wettability, and total surface energy measured by the sessile drop technique (Table 1). The determination of the surface free energy was performed using the Owens and Wendt Equation (1) (Owens and Wendt 1969).

$$\gamma_L(1+\cos\theta) = 2\left(\left(\gamma_L^d\gamma_S^d\right)^{1/2} + \left(\gamma_L^p\gamma_S^p\right)^{1/2}\right) \quad (1)$$

where γ_d and γ_p represent the dispersive and polar components of the liquid surface tension (γ_L), respectively. θ denotes the contact angle between the liquid (L) and the solid (S).

High-resolution field emission microscopy (Tescan MIRA with Field Emission Gun Schottky including Beam Deceleration Technology to enhance imaging performance at lower accelerating voltages) was utilized to characterize the passivation layer of the standard, citric acid-treated surfaces and the Piranha technique (Figure 2). Data were analyzed using SCA 20 software (Dataphysics). Three measurements were conducted for three different samples in each series.

2.2 | Protein Adsorption Assay

The protein adsorption capacity of the various implant surfaces was assessed using human plasma fibrinogen (Sigma-Aldrich, St. Louis, MO, USA) as a model protein. Each implant was vertically placed in an Eppendorf tube containing 0.5 mL of a buffered solution (NaCl 0.9%) with a protein concentration of 1.5 mg/mL. After 2 h of incubation at 37°C with agitation (75 r.p.m.), the implants were retrieved from the protein solution and rinsed with PBS to remove nonadherent proteins. Subsequently, the adsorbed proteins were extracted by incubating the implants with 0.5 mL of 1% sodium dodecyl sulfate (SDS) and sonicating for 10 min. The concentration of the extracted protein was quantified using a colorimetric micro bicinchoninic acid (BCA) assay kit (Cat. No. Ca15045; Thermo Scientific, Waltham, MA, USA).

2.3 | Bacterial Strains and Culture Conditions

The selected bacterial strains included *Streptococcus oralis* CECT 907T, *Veillonella parvula* NCTC 11810, *Actinomyces naeslundii* ATCC 19039, *Fusobacterium nucleatum* DMSZ 20482, *Aggregatibacter actinomycetemcomitans* DSMZ 8324, and *Porphyromonas gingivalis* ATCC 33277 (Sánchez et al. 2011). These species were cultivated on blood agar plates (Blood Agar Oxoid No 2; Oxoid, Basingstoke, UK), enriched with 5% (v/v) sterile horse blood (Oxoid), 5.0 mg/L hemin (Sigma), and 1.0 mg/L menadione (Merck, Darmstadt, Germany) under anaerobic conditions (10% H_2, 10% CO_2, and the remainder N_2) at 37°C for a duration of 24–72 h. Pure cultures of each bacterial strain were grown anaerobically for 24 h in a protein-rich medium based on modified brain heart infusion (BHI) (Becton, Dickinson and Company, Franklin

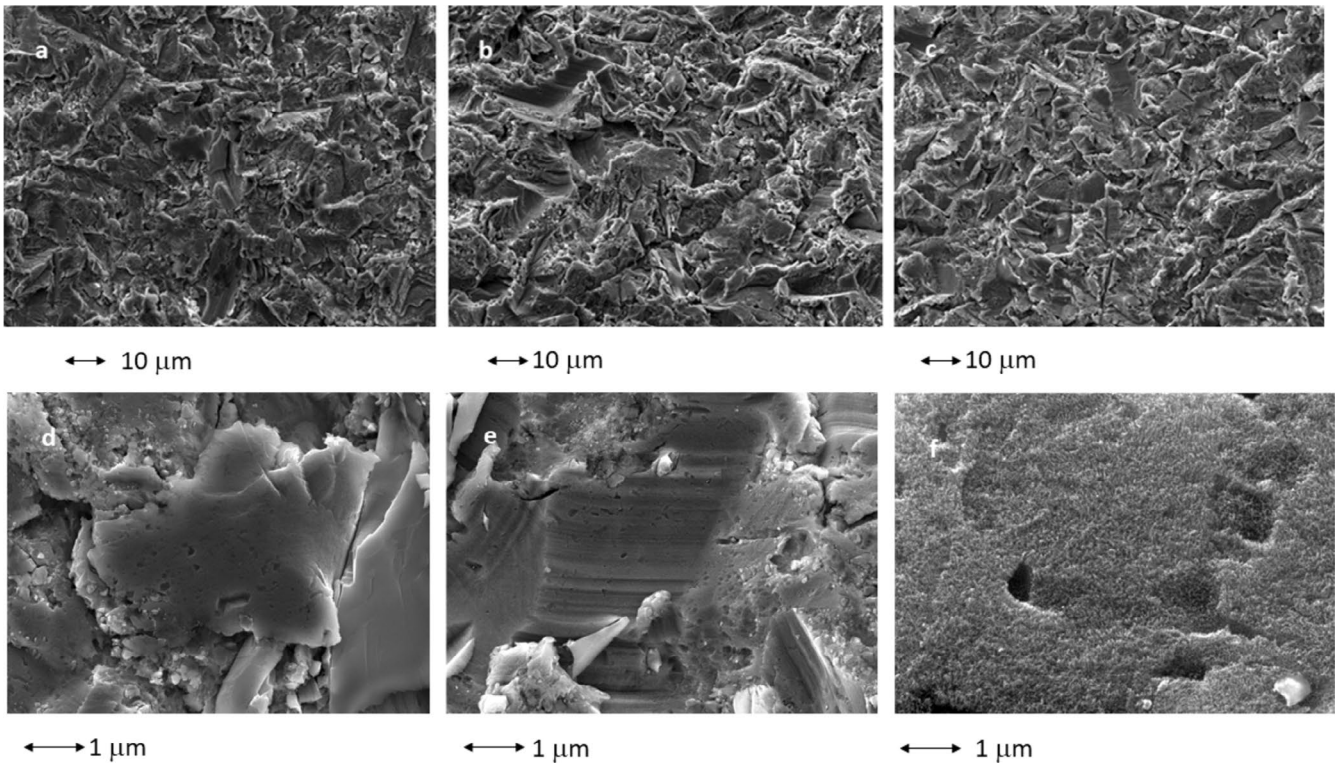

FIGURE 1 | Images obtained by scanning electron microscopy (SEM) with 500× magnification of the implant surfaces of the (a) standard, (b) citric acid and (c) piranha passivated implants. The lower row of images show (d) standard, (e) citric acid and (f) piranha implants at higher magnification ($n = 6$).

TABLE 1 | Values of roughness (Ra), contact angle (CA), surface free energy (SFE), and its dispersive (DISP) and polar (POL) components, for each surface treatment. Statistically significant differences marked as (a) versus standard and as (b) vs. citric acid ($p < 0.05$) ($n = 3$).

	Ra (nm)	CA (°)	SFE (mJ/m^2)	DISP (mJ/m^2)	POL (mJ/m^2)
Standard	149 ± 21	73.5 ± 7.2	40.8 ± 9.8	34.9 ± 3.3	7.5 ± 3.4
Citric acid	154 ± 32	38.6 ± 5.1a	65.7 ± 1.5 a	40.4 ± 0.2 a	25.3 ± 1.5 a
Piranha	159 ± 29	45.2 ± 6.6 a	71.2 ± 2.1 a, b	27.2 ± 1.1 a, b	44.0 ± 2.2 a, b

Lakes, NJ, USA). The medium was enriched with 2.5 g/L mucin (Oxoid), 1.0 g/L yeast extract (Oxoid), 0.1 g/L cysteine (Sigma), 2.0 g/L sodium bicarbonate (Merck), 5.0 mg/L hemin (Sigma), 1.0 mg/L menadione (Merck), and 0.25% (v/v) glutamic acid (Sigma). After incubation, bacterial growth was assessed via spectrophotometry at OD_{550} nm, and the cultures were adjusted to achieve a final concentration of 10^6 colony-forming units (CFU)/mL for all six bacterial strains.

2.4 | Biofilm Development

An in vitro dynamic biofilm model was utilized, comprising several key components (Sánchez et al. 2021). The system begins with a sterile source of modified BHI medium, which is transferred to the bioreactor containing the bacterial inoculum via a peristaltic pump operating at a constant pressure. This bioreactor (Lambda Minifor bioreactor, LAMBDA Laboratory Instruments, Baar, Switzerland) maintains the culture medium under controlled environmental conditions that replicate the oral cavity (37°C, pH 7.2, and an anaerobic atmosphere [10% H_2, 10% CO_2, and the balance N_2]). These conditions promote the growth of the bacterial mixture over specific time intervals. Using a peristaltic pump with a continuous flow rate of 30 mL/h, the bacterial mixture is directed to a custom-designed Robbins device. This device securely holds dental implants so that their surfaces are positioned within a flow channel, exposing the bacteria to controlled conditions and facilitating the formation of biofilms on the implant surfaces.

To evaluate the dynamics of biofilm formation on the implant surfaces, incubation times were set at 6, 12, and 24 h. Following this, the implants were removed from the Robbins device and assessed using the appropriate techniques. All experiments were carried out on separate days, each time utilizing fresh bacterial cultures. For qPCR analysis, experiments were performed in triplicate—three implants per surface type—across three independent biological replicates conducted on different days, resulting in a total of nine samples per time point ($n = 9$). For CLSM and SEM, two implants per surface type were used in each of the three independent experiments, also performed on

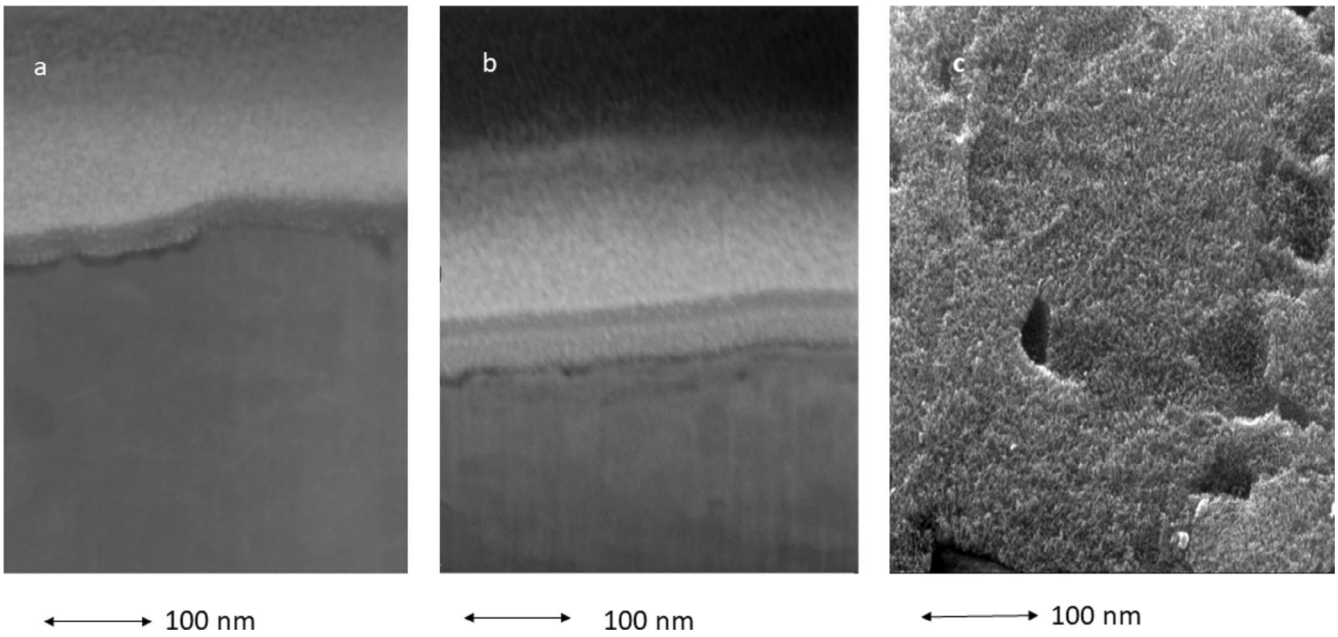

FIGURE 2 | Passivation layer of (a) standard, (b) citric acid passivated and (c) piranha passivated implants ($n = 6$).

separate days, resulting in six samples per time point ($n = 6$). For microscopic analyses, three representative images were taken from each implant using the corresponding technique.

2.5 | DNA Isolation and Quantitative Polymerase Chain Reaction (qPCR)

The implants extracted from the Robbins device were rinsed three times with 1.5 mL of PBS for 10 s each to remove nonadherent biofilm. Subsequently, they were placed in vials containing 1 mL of PBS and vortexed for 2 min at room temperature to disperse the biofilms. The resulting suspensions were centrifuged at 13,000 r.p.m. for 3 min, and DNA was extracted from the pelleted cells using an automated DNA extractor (Maxwell RSC Instrument, Promega, Madison, USA), along with its corresponding commercial kit (Maxwell RSC Genomic DNA Kit, Promega, Madison, USA). The extracted DNA was analyzed using qPCR to identify and quantify the bacterial species present in the biofilm model. Specific primers and probes targeting the 16S rRNA gene of each bacterial species were employed at optimal concentrations: *S. oralis*: 900, 900, and 300 nM; *A. naeslundii* and *P. gingivalis*: 300, 300, and 300 nM; *V. parvula*: 750, 750, and 400 nM; *A. actinomycetemcomitans*: 300, 300, and 200 nM; *F. nucleatum*: 600, 600, and 300 nM (Life Technologies Invitrogen and Applied Biosystems, Carlsbad, CA, USA; Roche Diagnostic GmbH, Mannheim, Germany). The primers and probes used were previously described (Sánchez et al. 2014). Amplification reactions were conducted in a 10 μL volume containing 5 μL of a 2 times master mix (LC 480 Probes Master, Roche). Negative control reactions were performed using 2.5 μL of sterile water as a no-template control (NTC) (Roche Diagnostic GmbH, Mannheim, Germany).

The qPCR protocol included an initial denaturation step at 95°C for 10 min, followed by 40 cycles of 95°C for 15 s and 60°C for 1 min. Amplification was carried out using a thermal cycler (LightCycler 480 II, Roche Diagnostic GmbH, Mannheim, Germany). The plates were sealed with QPCR Adhesive Clear Seals (4titude) using White FramStar 480 natural frame wells (4titude; The North Barn, Damphurst Lane, UK).

All DNA samples were analyzed in duplicate. The quantification cycle (Cq) values were determined using dedicated software (LC 480 Software 1.5, Roche Diagnostic GmbH, Mannheim, Germany), which automatically generated standard curves to convert Cq values into colony-forming units per milliliter (CFU/mL).

2.6 | Scanning Electron Microscope (SEM) Analysis for Studying the Morphology of Biofilms

Before microscopic analysis, the Robbins device was taken out of the bioreactor, and the implants were delicately retrieved. Each implant was rinsed three times with 1.5 mL of PBS for 10 s per rinse to remove unattached bacteria. The samples were fixed for 4 h at 4°C in a solution containing 4% paraformaldehyde (Panreac Química, Barcelona, Spain) and 2.5% glutaraldehyde (Panreac Química, Barcelona, Spain). After fixation, the implants were rinsed twice with sterile water for 10 min each. Subsequently, the samples were dehydrated using a gradient ethanol series of 30%, 50%, 70%, 80%, 90%, and 100%, with each step lasting 10 min. The dehydrated implants were dried at the critical point and coated with gold. The processed samples were examined using a JSM 6400 SEM (JSM6400, JEOL, Tokyo, Japan) equipped with a backscattered electron detector and operating at an image resolution of 25 kV. Observations were conducted at the National Centre of Electron Microscopy ICTS (Complutense University of Madrid, Madrid, Spain).

2.7 | Confocal Laser Scanning Microscopy (CLSM) Analysis for Studying Biofilm Vitality

A Leica LCS SP8 STED 3× confocal microscope (Mannheim, Germany) was utilized to image biofilms noninvasively. The

Leica Application Suite X software (version 3.5.7.23225) was set up to capture a *z*-series of scans (XYZ) with a thickness of 1 μm (8 bits, 512 × 512 pixels). For confocal analysis, representative areas of the implant surfaces were chosen, including both the peak of a thread and the base of the valleys. To visualize and quantify bacterial biofilms, the samples were stained with the LIVE/DEAD *Bac*Light bacterial viability kit solution (Molecular Probes, The Netherlands), which contains the nucleic acid dyes SYTO 9 and propidium iodide (PI). This technique differentiates cell viability: red fluorescence (PI) signifies dead cells with compromised membranes, while green fluorescence (SYTO 9) highlights live cells with intact membranes. The implants were coated with a 1:1 ratio of the fluorochromes and incubated for 9 ± 1 min to achieve optimal fluorescence signals at the appropriate wavelengths (SYTO 9: 515–530 nm; PI: > 600 nm). Following incubation, excess dye was removed by rinsing the implants in 1.5 mL of PBS for 10 s. The open-source tool Biofilm Viability Checker (Mountcastle et al. 2021) was employed to quantify the proportions of live and dead bacteria based on the maximum projection of the acquired images. The macro was refined to align more closely with the specific magnification conditions of our dataset. The analysis was conducted at the Biological Research Centre Margarita Salas (Centro de Investigaciones Biológicas, Consejo Superior de Investigaciones Científicas—CIB-CSIC), located at the Moncloa Campus of the Complutense University of Madrid (Madrid, Spain).

2.8 | Statistical Analysis

The selected outcome variables for comparing biofilms included the absorbed protein concentration from the protein adsorption assay (μg/mL), the bacterial counts for each species per biofilm (CFU mL^{-1}) derived from qPCR results, and the live/dead ratio obtained from CLSM images. Data are expressed as means and standard deviations (SD), and their normality was assessed using the Shapiro–Wilk test. A general linear model was developed to compare the bacterial counts for each bacterium. To compare the live/dead ratios from the CLSM data, a one-way ANOVA with Bonferroni's corrections for multiple comparisons was applied. Results were considered statistically significant at $p < 0.05$. All statistical analyses were performed using a software package (IBM SPSS Statistics 29.0; IBM Corporation, Armonk, NY, USA).

3 | Results

3.1 | Characterization of Material Specimens

Figure 2b illustrates the titanium oxide passivation layer on the citric acid-treated surfaces, which forms a smooth, homogeneous layer that mimics the surface topography. Figure 2c presents the nanostructure resulting from the Piranha treatments, where the oxide layer is no longer smooth but features titanium oxide nanopillars.

Table 1 depicts the roughness, contact angle values, and surface energy after the passivation treatments. While the roughness of the samples treated with citric acid and Piranha remained unchanged compared to the control surface, the contact angle values differed statistically significantly, exhibiting greater hydrophilicity. Additionally, total surface energy increased, particularly in the polar component.

3.2 | Protein Adsorption Assay

The results showed differences in the adsorption capacity among the three surfaces (Figure 3). Piranha-passivated implants displayed the lowest protein adsorption capacity (15.20 μg/mL) compared to the negative control (17.08 μg/mL) and the citric acid-passivated implants (20.01 μg/mL). However, the differences were not statistically significant.

3.3 | Quantitative Analysis by qPCR

All six bacterial species were detected by qPCR on the three types of implants tested at 6, 12, and 24 h. Figure 4 illustrates the dynamic formation of biofilms on the surfaces compared over these time points. When examining the primary colonizers (*A. naeslundii*, *V. parvula*, *S. oralis*) and the intermediate colonizer (*F. nucleatum*), lower bacterial concentrations were observed on the piranha-treated surface. After 24 h of incubation, bacterial counts for *V. parvula* and *A. naeslundii* on the piranha-treated surface were even lower than those on the negative control (citric acid) surface, with $\log_{10}$ values of 8.06 vs. 8.27 and 6.42 vs. 6.22, respectively. This trend was more pronounced for *S. oralis* and *F. nucleatum*.

Following the initial increase in bacterial colonization during the first 6–12 h, the bacterial counts plateaued. At 24 h, the counts were noticeably lower on the piranha-passivated implant compared to the citric acid-passivated implant, with *S. oralis* showing $\log_{10}$ values of 6.51 vs. 6.79 and *F. nucleatum* showing $\log_{10}$ values of 6.73 vs. 6.97, respectively. This is particularly significant for *F. nucleatum*, as it plays a crucial role in facilitating the colonization of more bacteria commonly associated with

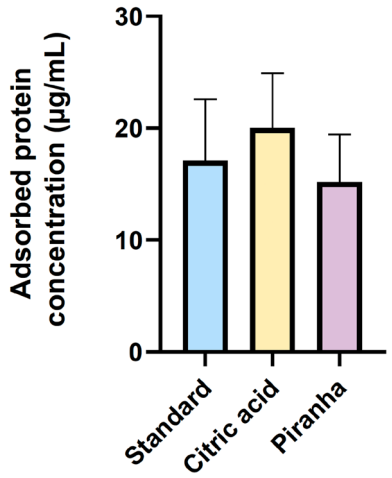

FIGURE 3 | Amount of fibrinogen protein adsorbed on the implant surfaces (represented as mean and standard deviation [SD] in μg/mL). No statistically significant differences were observed between groups ($p > 0.05$) ($n = 8$).

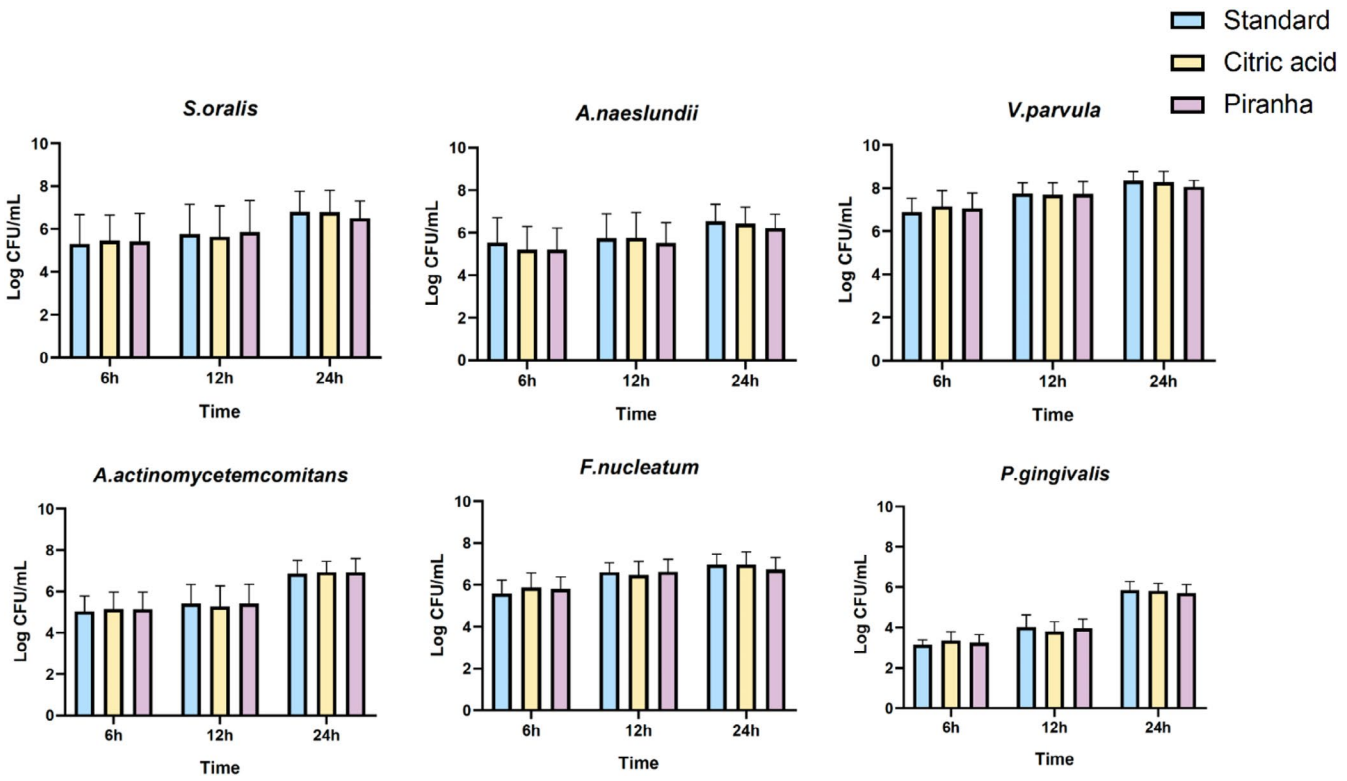

FIGURE 4 | Bacterial counts expressed as the decimal logarithm of colony-forming units ($\log_{10}$ CFU/mL) (represented as mean and standard deviation [SD] of colony-forming units [CFUs]/mL) of bacterial species, determined by quantitative polymerase chain reaction (qPCR) in 6-, 12- and 24-h biofilms formed on standard, citric acid and piranha passivated implants ($n = 9$), using specific primers and probes directed to the 16 rRNA. No statistically significant differences were observed between groups ($p > 0.05$) ($n = 9$).

peri-implant disease. However, none of the differences observed among the groups were statistically significant.

3.4 | SEM Analysis

Scanning electron microscope (SEM) images showing biofilm formation on standard, citric acid-treated, and piranha passivated implants were captured at 6, 12, and 24 h (Figure 5). At the 6-h mark, scattered coccoid bacterial colonies were observed on all three surfaces, although fewer bacteria were present on the piranha passivated implant compared to the others. By 12 h, bacterial colonization had significantly increased in the standard implants, and fusiform-shaped bacteria became more apparent, indicating progress in biofilm development. At 24 h, the biofilm structure became more complex, with a greater number of interwoven bacterial colonies. Nonetheless, some areas of the implants remained uncolonized. At this stage, no noticeable differences were observed among the three types of implants in terms of biofilm coverage or structural complexity.

3.5 | Confocal Laser Scanning Microscopy (CLSM)

Confocal laser scanning microscopy was used to capture images of biofilm formation on standard, citric acid-treated, and piranha passivated implants at 6-, 12-, and 24-h intervals. In the centre of the image, the peak of the dental implant is clearly visible, with the upper and lower valleys positioned to the left and right of the peak. This arrangement highlights the spatial distribution of the bacteria colonizing the implant surface (Figure 6). The Biofilm Viability Checker software (Mountcastle et al. 2021) was used to calculate the percentage of live and dead bacteria within the biofilm. As shown in Table 1, the percentage of dead bacteria increases over time, correlating with biofilm maturation. At 6 h, both citric acid-treated and piranha passivated implants exhibited a higher percentage of dead bacteria. However, at 12 and 24 h, piranha passivated implants consistently show a higher percentage of dead bacteria compared to citric acid-treated implants (Table 2).

4 | Discussion

This in vitro investigation has evaluated dental implants with a novel surface passivation method, "Piranha," in terms of its protein adsorption capabilities and effectiveness in inhibiting biofilm formation and viability on the implant surface compared to a negative control (standard titanium surface) and a positive control (titanium surface passivated with citric acid).

The Piranha treatments resulted in an oxide layer featuring titanium oxide nanopillars instead of the smooth, homogeneous titanium oxide passivation layer found on the citric acid-treated surfaces. The surface after the Piranha treatments was characterized by a spiky morphology, which likely contributes to the bactericidal effect, as the bacteria adsorbed on the surface are likely to be penetrated by these nanopillars. Although the passivation methods did not affect the surface roughness, the samples treated with citric acid and Piranha exhibited greater

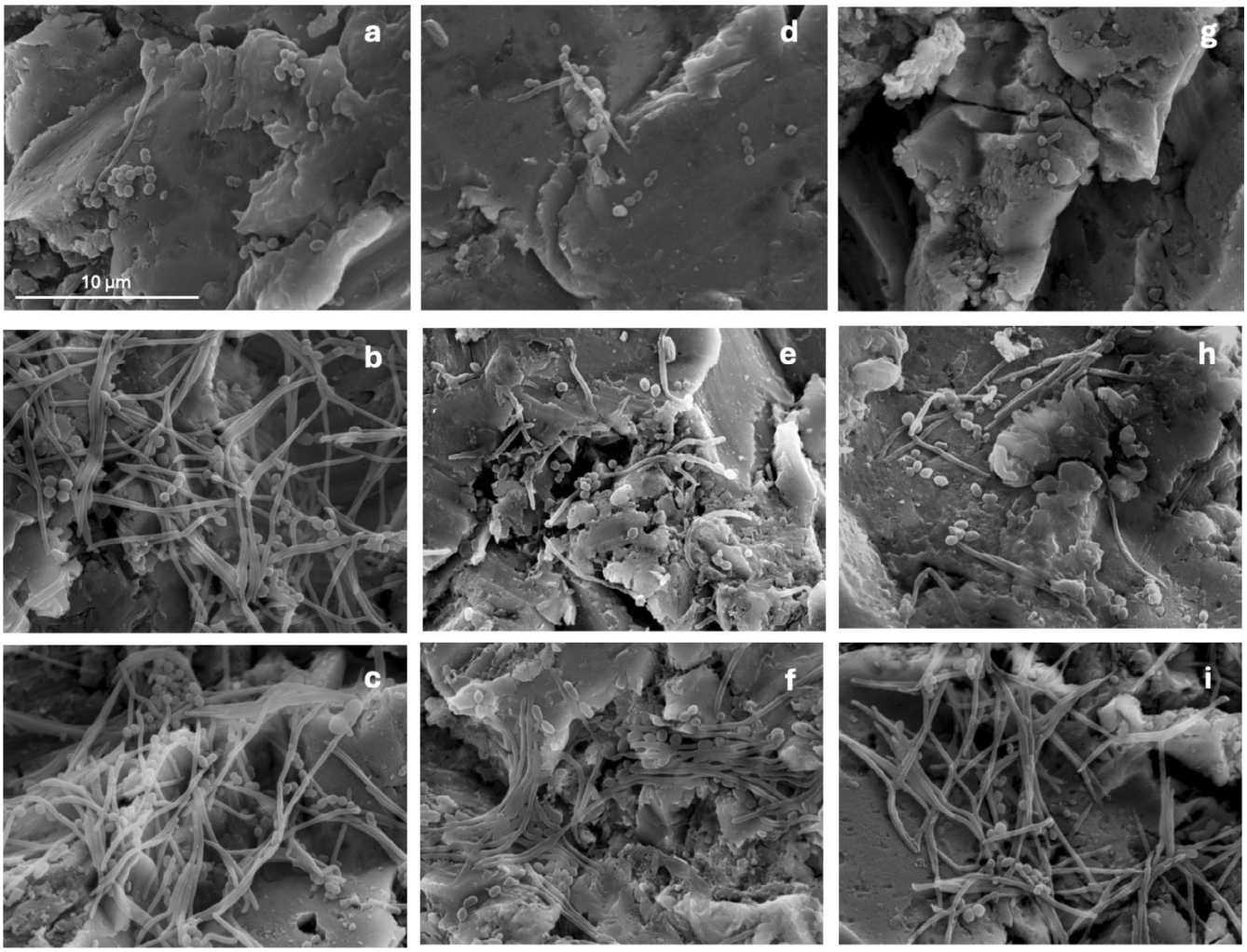

FIGURE 5 | Images obtained by scanning electron microscopy (SEM) with 5000× magnification of biofilms developed on standard implants (a–c), citric acid implants (d–f) and piranha passivated implants (g–i) at 6 h (a, d, g), 12 h (b, e, h) and 24 h (c, f, i) ($n = 6$).

hydrophilicity and elevated surface energy compared to the control, which may promote osteoblastic cell adhesion, proliferation, and differentiation (Harnett et al. 2007).

The protein adsorption assay was performed using fibrinogen as the model protein since this protein is derived from blood and biological fluids, which quickly adsorb onto implant surfaces and play a critical role in mediating cell adhesion (Barberi and Spriano 2021). The Piranha-treated surface exhibited the lowest capacity for fibrinogen adsorption compared to the citric acid-treated implant surface. These differences can be linked to the increased surface hydrophilicity resulting from passivation (Kujawa et al. 2023), as fibrinogen, being a large protein, tends to adsorb more easily onto hydrophobic surfaces due to stronger hydrophobic interactions (Wu et al. 2021). In contrast, citric acid passivation introduces carboxyl groups, leading to a negatively charged surface (Burel et al. 2021), which may enhance the binding of fibrinogen to negatively charged surfaces due to favorable electrostatic interactions (Zeliszewska et al. 2014). This differential adsorption of fibrinogen carries significant biological implications, as fibrinogen promotes bacterial adhesion by acting as a bridge between the biomaterial surface and specific bacterial adhesion receptors (Charville et al. 2008). Additionally, decreased fibrinogen adsorption may enhance biocompatibility by reducing the adhesion of platelets and monocytes/macrophages, which are key contributors to inflammatory responses on biomaterials (Horbett 2018; Hu et al. 2001).

To study bacterial colonization, this research utilized a validated in vitro multispecies biofilm model (Sánchez et al. 2011) to assess biofilm formation on titanium implants with three distinct surfaces: standard titanium surfaces, a newly developed passivated surface (Piranha), and citric acid passivated implants. Biofilm development was assessed at 6, 12, and 24 h to capture early bacterial adherence, which begins approximately 30 min after implant placement in the oral environment (Pokrowiecki et al. 2017). No statistically significant differences were found between standard and citric acid-treated implants for any bacteria at any time, based on bacterial counts determined through qPCR analysis. However, Piranha implants contained lower amounts of primary and intermediate colonizers. These findings align with a prior in vitro study (Cruz et al. 2022) showing reduced bacterial adhesion on piranha-passivated dental meshes compared to the control group. Yet, this study employed a mono-species model with a short incubation time that may not accurately represent mature biofilm status. Multiple studies have indicated that bacterial adhesion generally increases with greater surface hydrophobicity (Oh et al. 2018). Since

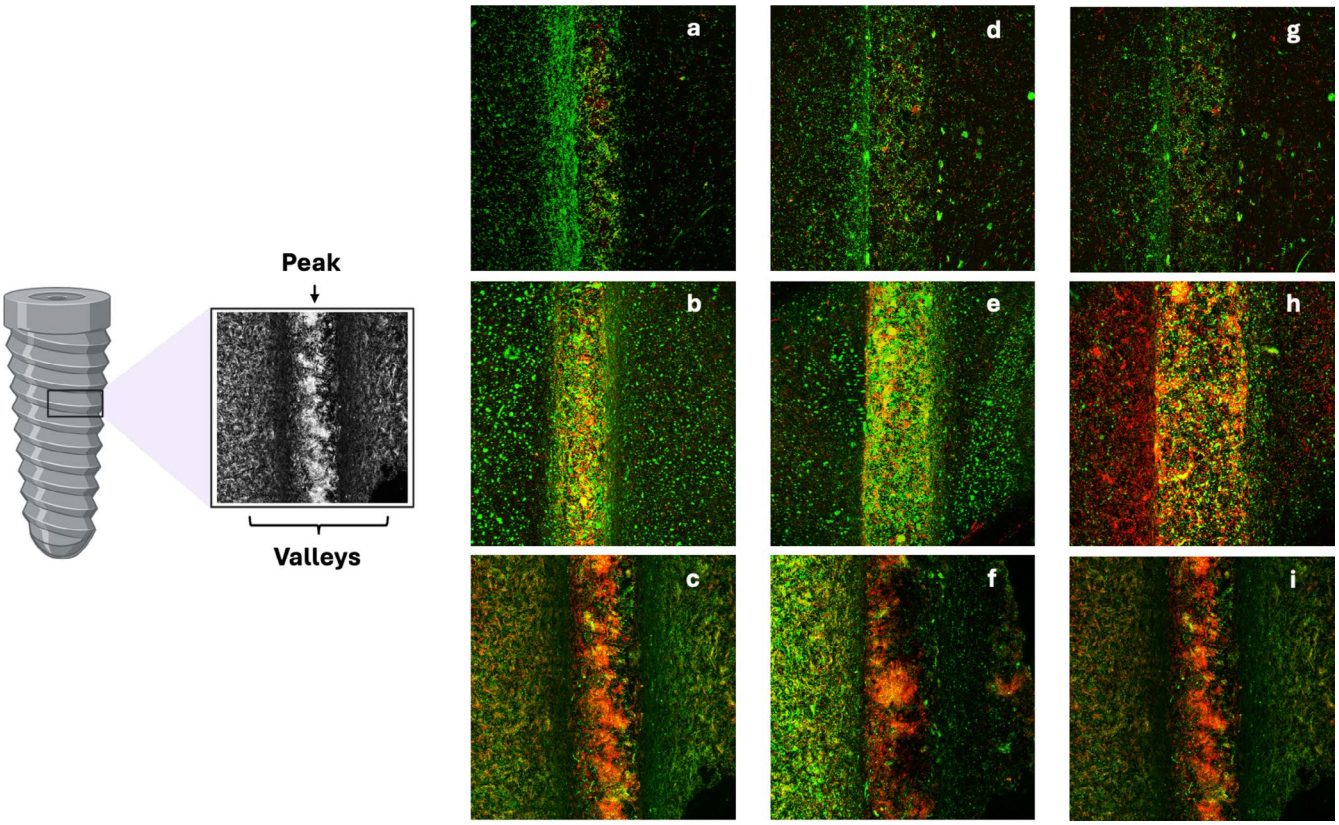

FIGURE 6 | Images obtained by confocal laser scanning microscopy (CLSM) of biofilms developed on standard implants (a–c), citric acid implants (d–f) and piranha passivated implants (g–i) at 6 h (a, d, g), 12 h (b, e, h) and 24 h (c, f, i). LIVE/DEAD *Bac*Light was used. Live bacteria (green) and dead bacteria (red). The images were generated using maximum intensity projections of the confocal *z*-stacks ($n = 6$).

TABLE 2 | Percentage of dead bacteria in biofilms (mean ± SD): analysis of 6-, 12-, and 24-h biofilms on standard, citric acid, and piranha-passivated implants using CLSM and LIVE/DEAD *Bac*Light Staining. No statistically significant differences were observed between groups ($p > 0.05$) ($n = 6$).

Incubation time (h)	Implant group	Mean percentage of dead bacteria (%)	SD
6	Standard	14.3	15.1
	Citric acid	27.3	29.2
	Pirahna	36.2	28.8
12	Standard	51.1	26.5
	Citric acid	44.3	16.6
	Pirahna	63.1	28.0
24	Standard	55.6	16.6
	Citric acid	44.9	34.0
	Pirahna	63.6	21.9

Piranha treatment enhances surface hydrophilicity (Kujawa et al. 2023), it is expected to decrease bacterial adhesion while promoting cell adhesion and proliferation, as hydrophilic surfaces are known to encourage these biological interactions (Klein et al. 2013). This dual benefit makes Piranha-treated surfaces particularly promising for dental implants, as they not only reduce bacterial colonization but may also support tissue integration. In contrast, citric acid-passivated implants showed lower bacterial counts for *A. naeslundii* at 6 and 24 h, and for *P. gingivalis* at 12 h compared to the standard group. However, no statistically significant differences were found. The bactericidal effect of citric passivation has been previously described, albeit using a simpler mono-species model with a short incubation time (Punset et al. 2021). This aligns with an earlier study that utilized a multispecies oral biofilm model, in which the citric acid-passivated surface displayed almost no significant differences compared to the other surfaces tested (Vilarrasa et al. 2023). The bactericidal effectiveness of the surface significantly depends on the concentration of citric acid used during the passivation process. While higher concentrations reduce bacterial adhesion more effectively, they also lead to increased ion release, raising toxicity concerns and rendering them less favorable (Verdeguer et al. 2022). SEM analysis further supported these findings, indicating that the implant surface covered by biofilm increased over time in a similar manner across all three surfaces. At 6 h, predominantly coccoid bacterial colonies were observed, with Piranha-passivated implants exhibiting fewer of them. Since primary colonizers typically display a coccoid shape, this finding correlates with the lower qPCR counts detected on these implants. As the biofilm matured, the number of fusiform-shaped bacteria increased, coinciding with a rise in biofilm complexity. In terms of CLSM images, Piranha implants retained their antimicrobial efficacy over time, while

citric acid implants appeared to be less effective at sustaining bacterial reduction during the later stages of biofilm development. The antimicrobial effectiveness of citric acid implants is closely linked to the pH and concentration of its various ionized forms. It is believed that under low pH conditions, citric acid can penetrate microbial membranes, cause acidification of the intracellular environment, and lead to structural damage to the cell (Burel et al. 2021). Citric acid has been shown to be effective in eliminating bacteria at the core of biofilm colonies, but it is ineffective against cells located at the biofilm periphery (Kundukad et al. 2020). As the biofilm matures and produces bacterial exopolysaccharides (EPS), these substances can obstruct or reduce contact between citric acid and the bacterial cells (Liu et al. 2024). This may explain the persistence of viable bacteria over prolonged periods of growth. The antibacterial effect of Piranha implants is likely due to their surface topography, mainly caused by spike-like nanopillar nanostructures that can mechanically break down the bacterial murein wall, especially in Gram-negative bacteria with thin peptidoglycan layers (Jenkins et al. 2020). However, this potential mechanism cannot be proven by the results of this investigation, as we did not observe a significant increase in dead bacteria on Piranha-treated surfaces compared to the other implant surface groups at the 6-h evaluation period. Additionally, since the early colonizers are primarily Gram-positive species, such as *streptococci* and *actinomyces*, which have thicker cell walls and may be less susceptible to mechanical disruption, the direct bactericidal effect of the nanopillars during initial biofilm formation is likely limited. The antimicrobial action of Piranha implants, along with their mechanical impact (Jenkins et al. 2020), may function by stimulating an increase in Reactive Oxygen Species (ROS) production, similar to the mechanisms by which bactericidal antibiotics operate (Kohanski et al. 2007). Additionally, TiO_2 nanotubes have been shown to promote fibroblast proliferation, establishing them as a beneficial framework for dental implants (Dias-Netipanyj et al. 2020; Xu et al. 2020). This indicates that Piranha-treated implants are a promising option since reducing the viability of bacterial cells during the initial adhesion stage can help prevent biofilm formation (Ma et al. 2022) and diminish the risk of peri-implantitis.

5 | Conclusions

The findings from this investigation show trends toward reduced fibrinogen adsorption, lower total bacterial counts, and decreased bacterial viability on the Piranha-treated surface in vitro; however, these differences were not statistically significant. Although these findings suggest a potential benefit of the Piranha treatment for dental implants, further investigation is needed to reach conclusive results. However, the results of this study should be interpreted cautiously due to significant limitations in the in vitro experimental design. Samples were not coated with saliva, as there is no consensus on its impact on bacterial colonization. This allowed us to isolate the influence of surface characteristics without introducing additional variables. Another limitation of this investigation may be the use of sonication as a reliable method to detach proteins and/or bacteria from the implant surfaces. Although this technique is widely used and accepted in the literature, its effectiveness in fully recovering surface-adhered material has not been conclusively validated. Therefore, the reported results may underestimate the actual amounts present. Nonetheless, since all surfaces were processed using the same protocol, the relative comparisons between groups remain valid. As a result, the findings may not be fully extrapolable to the clinical context, where salivary pellicle formation occurs naturally. Therefore, further research is necessary to validate the effectiveness of the Piranha passivation method. Clinical trials should assess its performance in practical scenarios alongside foundational research studies to clarify its underlying mechanisms of action.

Author Contributions

Paula Nuevo: methodology, investigation, writing – original draft, data curation. **Leire Virto:** conceptualization, methodology, investigation, writing – review and editing, data curation, formal analysis. **Honorato Ribeiro-Vidal:** writing – review and editing, supervision, data curation, investigation. **Javier Gil:** conceptualization, investigation, writing – review and editing, formal analysis. **Mariano Sanz:** conceptualization, supervision, project administration, writing – review and editing, funding acquisition.

Acknowledgments

We would like to thank the technical support of Dr. A.M. Vicente at the ICTS National Centre of Electron Microscopy (University Complutense, Madrid, Spain), M.G. Elvira, M.D. Hernández, and M.T. Seisdedos at the Confocal and Fluorescence Microscopy Service of Margarita Salas Biological Research Center (Superior Center for Scientific Research) and R. Ayuso and J.E. Verdasco at the Platform of Mechanic Workshops (University Complutense, Madrid, Spain). The authors are also grateful to the Spanish Government for its support through the research project MINECO (PID2022-137496OB-I00).

Conflicts of Interest

The authors declare no conflicts of interest.

Data Availability Statement

The data that support the findings of this study are available from the corresponding author upon reasonable request.

References

Barberi, J., and S. Spriano. 2021. "Titanium and Protein Adsorption: An Overview of Mechanisms and Effects of Surface Features." *Materials* 14: 1590. https://doi.org/10.3390/ma14071590.

Belibasakis, G. N., G. Charalampakis, N. Bostanci, and B. Stadlinger. 2015. "Peri-Implant Infections of Oral Biofilm Etiology." *Advances in Experimental Medicine and Biology* 830: 69–84. https://doi.org/10.1007/978-3-319-11038-7_4.

Burel, C., A. Kala, and L. Purevdorj-Gage. 2021. "Impact of pH on Citric Acid Antimicrobial Activity Against Gram-Negative Bacteria." *Letters in Applied Microbiology* 72, no. 3: 332–340. https://doi.org/10.1111/lam.13420.

Busscher, H. J., M. Rinastiti, W. Siswomihardjo, and H. C. Van Der Mei. 2010. "Biofilm Formation on Dental Restorative and Implant Materials." *Journal of Dental Research* 89: 657–665. https://doi.org/10.1177/0022034510368644.

Charville, G. W., E. M. Hetrick, C. B. Geer, and M. H. Schoenfisch. 2008. "Reduced Bacterial Adhesion to Fibrinogen-Coated Substrates via Nitric Oxide Release." *Biomaterials* 29, no. 30: 4039–4044. https://doi.org/10.1016/j.biomaterials.2008.07.005.

Chatzopoulos, G. S., and L. F. Wolff. 2024. "Survival Rate of Implants Performed at Sites of Previously Failed Implants and Factors Associated With Failure: A Retrospective Investigation." *Journal of Dental Sciences* 19, no. 3: 1741–1747. https://doi.org/10.1016/j.jds.2023.10.012.

Cruz, N., J. Gil, M. Punset, et al. 2022. "Relevant Aspects of Piranha Passivation in Ti6Al4V Alloy Dental Meshes." *Coatings* 12, no. 2: 154. https://doi.org/10.3390/coatings12020154.

Cruz, N., M. I. Martins, J. D. Santos, J. G. Mur, and J. P. Tondela. 2020. "Surface Comparison of Three Different Commercial Custom-Made Titanium Meshes Produced by SLM for Dental Applications." *Materials* 13, no. 9: 2177. https://doi.org/10.3390/ma13092177.

Dias-Netipanyj, M. F., L. Sopchenski, T. Gradowski, S. Elifio-Esposito, K. C. Popat, and P. Soares. 2020. "Crystallinity of TiO_2 Nanotubes and Its Effects on Fibroblast Viability, Adhesion, and Proliferation." *Journal of Materials Science: Materials in Medicine* 31, no. 11: 94. https://doi.org/10.1007/s10856-020-06431-4.

Diaz, P., E. Gonzalo, L. J. G. Villagra, B. Miegimolle, and M. J. Suarez. 2022. "What Is the Prevalence of Peri-Implantitis? A Systematic Review and Meta-Analysis." *BMC Oral Health* 22, no. 1: 449. https://doi.org/10.1186/s12903-022-02493-8.

Esteves, G. M., J. Esteves, M. Resende, L. Mendes, and A. S. Azevedo. 2022. "Antimicrobial and Antibiofilm Coating of Dental Implants—Past and New Perspectives." *Antibiotics* 11: 235. https://doi.org/10.3390/antibiotics11020235.

Fragkioudakis, I., G. Tseleki, A. E. Doufexi, and D. Sakellari. 2021. "Current Concepts on the Pathogenesis of Peri-Implantitis: A Narrative Review." *European Journal of Dentistry* 15: 379–387. https://doi.org/10.1055/s-0040-1721903.

Harnett, E. M., J. Alderman, and T. Wood. 2007. "The Surface Energy of Various Biomaterials Coated With Adhesion Molecules Used in Cell Culture." *Colloids and Surfaces B: Biointerfaces* 55, no. 1: 90–97. https://doi.org/10.1016/j.colsurfb.2006.11.021.

Horbett, T. A. 2018. "Fibrinogen Adsorption to Biomaterials." *Journal of Biomedical Materials Research – Part A* 106: 2777–2788. https://doi.org/10.1002/jbm.a.36460.

Hu, W.-J., J. W. Eaton, and L. Tang. 2001. "Molecular Basis of Biomaterial-Mediated Foreign Body Reactions." *Blood* 98: 1231–1238.

Jenkins, J., J. Mantell, C. Neal, et al. 2020. "Antibacterial Effects of Nanopillar Surfaces Are Mediated by Cell Impedance, Penetration and Induction of Oxidative Stress." *Nature Communications* 11, no. 1: 1626. https://doi.org/10.1038/s41467-020-15471-x.

Klein, M. O., A. Bijelic, T. Ziebart, et al. 2013. "Submicron Scale-Structured Hydrophilic Titanium Surfaces Promote Early Osteogenic Gene Response for Cell Adhesion and Cell Differentiation." *Clinical Implant Dentistry and Related Research* 15, no. 2: 166–175. https://doi.org/10.1111/j.1708-8208.2011.00339.x.

Kohanski, M. A., D. J. Dwyer, B. Hayete, C. A. Lawrence, and J. J. Collins. 2007. "A Common Mechanism of Cellular Death Induced by Bactericidal Antibiotics." *Cell* 130, no. 5: 797–810. https://doi.org/10.1016/j.cell.2007.06.049.

Kujawa, J., S. Al-Gharabli, and W. Kujawski. 2023. "Ceramic Membranes Activation via Piranha Reagent – A Facile Way for Significant Enhancement in Membrane Performance." *Chemical Engineering Journal* 471: 144497. https://doi.org/10.1016/j.cej.2023.144497.

Kundukad, B., G. Udayakumar, E. Grela, et al. 2020. "Weak Acids as an Alternative Anti-Microbial Therapy." *Biofilm* 2: 100019. https://doi.org/10.1016/j.bioflm.2020.100019.

Kunrath, M. F., C. Garaicoa-Pazmino, P. M. Giraldo-Osorno, et al. 2024. "Implant Surface Modifications and Their Impact on Osseointegration and Peri-Implant Diseases Through Epigenetic Changes: A Scoping Review." *Journal of Periodontal Research* 59: 1095–1114. https://doi.org/10.1111/jre.13273.

Lang, N. P., and T. Berglundh. 2011. "Periimplant Diseases: Where Are We Now? – Consensus of the Seventh European Workshop on Periodontology." *Journal of Clinical Periodontology* 38, no. Suppl. 11: 178–181. https://doi.org/10.1111/j.1600-051X.2010.01674.x.

Lee, A., and H. L. Wang. 2010. "Biofilm Related to Dental Implants." *Implant Dentistry* 19, no. 5: 387–393. https://doi.org/10.1097/ID.0b013e3181effa53.

Lee, C. T., Y. W. Huang, L. Zhu, and R. Weltman. 2017. "Prevalences of Peri-Implantitis and Peri-Implant Mucositis: Systematic Review and Meta-Analysis." *Journal of Dentistry* 62: 1–12. https://doi.org/10.1016/j.jdent.2017.04.011.

Liu, H. Y., E. L. Prentice, and M. A. Webber. 2024. "Mechanisms of Antimicrobial Resistance in Biofilms." *Npj Antimicrobials and Resistance* 2, no. 1: 27. https://doi.org/10.1038/s44259-024-00046-3.

Ma, R., X. Hu, X. Zhang, et al. 2022. "Strategies to Prevent, Curb and Eliminate Biofilm Formation Based on the Characteristics of Various Periods in One Biofilm Life Cycle." *Frontiers in Cellular and Infection Microbiology* 12: 1003033. https://doi.org/10.3389/fcimb.2022.1003033.

Mountcastle, S. E., N. Vyas, V. M. Villapun, et al. 2021. "Biofilm Viability Checker: An Open-Source Tool for Automated Biofilm Viability Analysis From Confocal Microscopy Images." *npj Biofilms and Microbiomes* 7, no. 1: 44. https://doi.org/10.1038/s41522-021-00214-7.

Oh, J. K., Y. Yegin, F. Yang, et al. 2018. "The Influence of Surface Chemistry on the Kinetics and Thermodynamics of Bacterial Adhesion." *Scientific Reports* 8, no. 1: 17247. https://doi.org/10.1038/s41598-018-35343-1.

Owens, D. K., and R. C. Wendt. 1969. "Estimation of the Surface Free Energy of Polymers." *Journal of Applied Polymer Science* 13: 1741–1747.

Pokrowiecki, R., A. Mielczarek, T. Zaręba, and S. Tyski. 2017. "Oral Microbiome and Peri-Implant Diseases: Where Are We Now?" *Therapeutics and Clinical Risk Management* 13: 1529–1542. https://doi.org/10.2147/TCRM.S139795.

Punset, M., J. Villarrasa, J. Nart, et al. 2021. "Citric Acid Passivation of Titanium Dental Implants for Minimizing Bacterial Colonization Impact." *Coatings* 11, no. 2: 1–13. https://doi.org/10.3390/coatings11020214.

Rokaya, D., V. Srimaneepong, W. Wisitrasameewon, M. Humagain, and P. Thunyakitpisal. 2020. "Peri-Implantitis Update: Risk Indicators, Diagnosis, and Treatment." *European Journal of Dentistry* 14: 672–682. https://doi.org/10.1055/s-0040-1715779.

Sánchez, M. C., A. Alonso-Español, H. Ribeiro-Vidal, B. Alonso, D. Herrera, and M. Sanz. 2021. "Relevance of Biofilm Models in Periodontal Research: From Static to Dynamic Systems." *Microorganisms* 9: 1–20. https://doi.org/10.3390/microorganisms9020428.

Sánchez, M. C., A. Llama-Palacios, V. Blanc, R. León, D. Herrera, and M. Sanz. 2011. "Structure, Viability and Bacterial Kinetics of an In Vitro Biofilm Model Using Six Bacteria From the Subgingival Microbiota." *Journal of Periodontal Research* 46, no. 2: 252–260. https://doi.org/10.1111/j.1600-0765.2010.01341.x.

Sánchez, M. C., A. Llama-Palacios, E. Fernández, et al. 2014. "An In Vitro Biofilm Model Associated to Dental Implants: Structural and Quantitative Analysis of In Vitro Biofilm Formation on Different Dental Implant Surfaces." *Dental Materials* 30, no. 10: 1161–1171. https://doi.org/10.1016/j.dental.2014.07.008.

Verdeguer, P., J. Gil, M. Punset, et al. 2022. "Citric Acid in the Passivation of Titanium Dental Implants: Corrosion Resistance and Bactericide Behavior." *Materials* 15, no. 2: 545. https://doi.org/10.3390/ma15020545.

Vilarrasa, J., G. Àlvarez, A. Soler-Ollé, J. Gil, J. Nart, and V. Blanc. 2023. "Bacterial Adhesion of TESPSA and Citric Acid on Different Titanium Surfaces Substrate Roughness: An In Vitro Study With a Multispecies

Oral Biofilm Model." *Materials* 16, no. 13: 4592. https://doi.org/10.3390/ma16134592.

Vilarrasa, J., C. Pereira Couto, G. Àlvarez, et al. 2025. "Microbiological, Inflammatory and Clinical Outcome of Citric Acid Passivated Definitive Abutments: Interim 12-Month Results From a Randomised Controlled Clinical Trial." *Journal of Clinical Periodontology* 52: 813–825. https://doi.org/10.1111/jcpe.14146.

Wu, X., C. Wang, P. Hao, F. He, Z. Yao, and X. Zhang. 2021. "Adsorption Properties of Albumin and Fibrinogen on Hydrophilic/Hydrophobic TiO_2 Surfaces: A Molecular Dynamics Study." *Colloids and Surfaces B: Biointerfaces* 207: 111994. https://doi.org/10.1016/j.colsurfb.2021.111994.

Xu, Z., Z. Xu, Y. He, et al. 2020. "Enhanced Human Gingival Fibroblast Response and Reduced *Porphyromonas gingivalis* Adhesion With Titania Nanotubes." *BioMed Research International* 2020: 5651780. https://doi.org/10.1155/2020/5651780.

Zeliszewska, P., A. Bratek-Skicki, Z. Adamczyk, and M. Cieśla. 2014. "Human Fibrinogen Adsorption on Positively Charged Latex Particles." *Langmuir* 30, no. 37: 11165–11174. https://doi.org/10.1021/la5025668.

Zhai, S., Y. Tian, X. Shi, et al. 2023. "Overview of Strategies to Improve the Antibacterial Property of Dental Implants." *Frontiers in Bioengineering and Biotechnology* 11: 1267128. https://doi.org/10.3389/fbioe.2023.1267128.